ARTICLES

Ultrafast Decarboxylation of Carbonyloxy Radicals: Influence of Molecular Structure

Bernd Abel, Jens Assmann, Michael Buback, Christian Grimm, Matthias Kling,* Stefan Schmatz, Jörg Schroeder, and Thomas Witte

Institut für Physikalische Chemie, Universität Göttingen, Tammannstrasse 6, 37077 Göttingen, Germany

Received: April 22, 2003; In Final Form: August 27, 2003

Experimental and theoretical investigations on the ultrafast photoinduced decomposition of three *tert*-butyl peroxides of general structure R−C(O)O−O−*tert*-butyl with R = phenyloxy, benzyl, or naphthyloxy in solution are presented. Photoinduced O−O bond scission occurs within the time resolution (200 fs) of the pump−probe experiment. The subsequent dissociation of photochemically excited carbonyloxy radicals, $R-CO_2$, has been monitored on a picosecond time scale by transient absorption at wavelengths between 290 and 1000 nm. The measured decay of $R-CO_2$ is simulated via statistical unimolecular rate theory using molecular energies, geometries, and vibrational frequencies obtained from density functional theory (DFT) calculations. The results are compared with recent data for *tert*-butyl peroxybenzoate (R = phenyl). While benzoyloxy radicals exhibit nanosecond to microsecond lifetimes at ambient temperature, insertion of an oxygen atom or a methylene group between the phenyl or naphthyl chromophore and the CO_2 moiety significantly decreases the stability and thus lowers the lifetime of the carbonyloxy radicals in solution to picoseconds. The reasons behind this structural effect on decomposition rate are discussed in terms of barrier heights for decarboxylation on the ground-state potential energy surface and of a fast reaction channel via electronically excited states of carbonyloxy radicals. Arrhenius parameters are reported for thermal rate constants, $k(T)$, of $R-CO_2$ decarboxylation as deduced from modeling of the time-resolved experimental data in conjunction with the DFT calculations.

I. Introduction

Organic peroxides belong to a group of compounds of fundamental as well as of application-oriented interest due to their extensive use as initiators in free-radical polymerizations.[1−4] The time scale of peroxide decomposition in different solvents and the dynamics of active intermediates affect both initiation rate and efficiency.[4,5] To optimize the initiation efficiency, a thorough understanding of the influence of peroxide structure on fragmentation dynamics and kinetics is required. A large body of literature has accumulated on the thermal decomposition of organic peroxides,[2,4] among which *tert*-butyl peroxides and peroxyesters have been investigated in considerable detail.

The mechanism of peroxide decarboxylation, that is, whether bond breaking in peroxyesters, diacyl peroxides, or peroxycarbonates occurs in a stepwise (sequential) or a concerted fashion, is of particular interest. This aspect has been addressed by several groups.[6−12] The question about the mechanism is obviously related to the time scale of observation. On the basis of thermal experiments, concerted bond breaking and stepwise dissociation via intermediate radicals on a picosecond or nanosecond time scale cannot be safely distinguished. Therefore, highly time-resolved (subpicosecond) studies are required to understand the decarboxylation mechanism in more detail.[13,14]

Studies on photochemical decomposition of organic peroxides by means of microsecond and nanosecond flash photolysis in conjunction with visible absorption or electron paramagnetic resonance (EPR) spectroscopy[15−22] have revealed that intermediate aroyloxy radicals are involved in the decomposition of diaroyl peroxides. *tert*-Butyl peroxides such as *tert*-butyl peroxybenzoate and *tert*-butyl peroxy-4-methoxy-benzoate were found to release the same reactive intermediates as the corresponding diaroyl peroxides, that is, benzoyloxy and 4-methoxybenzoyloxy radicals, respectively.[15,22] Investigations on substituted aroyloxy radicals revealed nanosecond to microsecond lifetimes,[17] in keeping with the observation of aroyloxy end groups in polymers produced in reactions with dibenzoyl peroxide being applied as initiator.[23] However, the reason behind the significantly different photodissociation quantum yields of aroyloxy radicals from aromatic *tert*-butyl peroxyesters and diaroyl peroxides[15,22] remained unclear.

Intermediate radicals from light-induced decomposition of *tert*-butyl peroxyesters were also identified in experiments with nanosecond to picosecond time resolution.[15,22,24−26] Kochi and co-workers studied the decarboxylation of carbonyloxy radicals after photogeneration via electron donor−acceptor complexes by femtosecond visible spectroscopy.[27,28] However, insufficient time resolution or spectral overlap prevented a detailed insight into the dissociation mechanism in prior studies. In particular, the dependence of the dynamics on molecular structure, internal

* Corresponding author. Present address: Department of Chemistry, University of California, Berkeley, D90 Hildebrand Hall, Berkeley, California 94720. E-mail: mkling@uclink.berkeley.edu.

10.1021/jp0350823 CCC: $25.00
Published on Web 10/22/2003

SCHEME 1: Scheme of Sequential Dissociation for UV Photoinduced Decomposition of *tert*-Butyl Peroxyesters with R = Phenyl or Naphthyl and X = O or CH_2

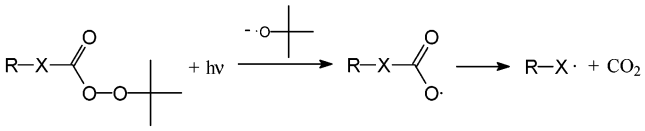

energy distribution, and solvent environment is not adequately understood so far.[4,5]

In recent studies with picosecond to femtosecond time resolution, we directly observed the formation and decarboxylation of intermediate aroyloxy radicals[13,29] and the formation of aryl radicals and CO_2 upon photoinduced decomposition of *tert*-butyl peroxyesters and diaroyl peroxides.[5,30,31] The results of these experiments clearly show that peroxide photofragmentation occurs as a fast *sequential* process, in which the primary step, that is, the breaking of the O−O single bond, takes place on a subpicosecond time scale.[5,13,30,31] Thus the mechanism anticipated on the basis of intuitive chemical arguments, in particular, on the different nature of chemical bonds and bond energies, is confirmed.[32] These studies further demonstrate that the average lifetime of aroyloxy radicals is significantly reduced in the case that these radicals are produced in an electronically excited state or in the electronic ground state with considerable vibrational excess energy. Taking this finding into account, we recently proposed a model for the two-step sequential dissociation of organic peroxides based on molecular parameters taken from both experiments and quantum-chemical calculations.

The decarboxylation of aroyloxy radicals is considered to consist of two processes: (i) the fast direct reaction from an electronically excited state and (ii) the fragmentation in the electronic ground state. The rate of the latter process is strongly affected by the rate of vibrational cooling via coupling to the bath modes. The vibrational energy transfer to the solvent environment has been included in our model in a heuristic manner. We were able to adequately represent and understand benzoyloxy radical decarboxylation over the femtosecond to microsecond time range, as well as differences in quantum yields of benzoyloxy radicals from decomposition of *tert*-butyl peroxybenzoate and of dibenzoyl peroxide.[29]

In extension of the preceding work, the present paper addresses photoinduced dissociation dynamics of peroxides of general structure R−X−C(O)O−O−*tert*-butyl, with R = phenyl or naphthyl and X = O or CH_2. In Scheme 1, the general decomposition mechanism is given. The primary photodissociation of the parent peroxide molecule yields the R−X−CO_2/*tert*-butoxy radical pair. Subsequent decarboxylation of R−X−CO_2 produces the radical R−X and CO_2.

The peroxides under investigation are *tert*-butyl peroxyphenyl carbonate (TBPPC), *tert*-butyl peroxyphenylacetate (TBPPA), and *tert*-butyl 2-peroxynaphthyl carbonate (TBNC). The kinetic results will be compared with recent data on *tert*-butyl peroxybenzoate (TBPB).[13] The four peroxides are displayed in Scheme 2.

The primary interest of the present study focuses on the structural effect of the isolobal bridging groups between the ring chromophore and the CO_2 moiety. Electronic delocalization decreases in going from TBPB to the systems TBPPC and TBPPA. Comparison of the decomposition rates of TBPPC and TBNC will afford studying the dependence of the kinetics on the size of the aromatic chromophore. The formation of intermediate radicals and their decarboxylation is monitored with femtosecond time resolution. The decarboxylation of carbonyloxy radicals will be analyzed with a model that has already been applied for the quantitative description of decarboxylation of benzoyloxy and naphthoyloxy radicals from photolysis of TBPB[13] and of di(1-naphthoyl) peroxide,[29] respectively. The application of experimental and theoretical methods in conjunction with the kinetic modeling of highly time-resolved concentration versus time profiles is the key toward the understanding of reaction mechanisms and time scales.

SCHEME 2: Chemical Structures and Abbreviations of *tert*-Butyl Peroxide Compounds Studied within the Present Work, *tert*-Butyl Peroxyphenyl Carbonate (TBPPC), *tert*-Butyl Peroxyphenylacetate (TBPPA), *tert*-Butyl 2-Peroxynaphthyl Carbonate (TBNC), and *tert*-Butyl Peroxybenzoate (TBPB)[a]

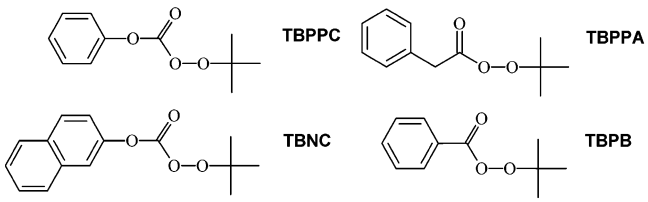

[a] While TBPPC, TBPPA, and TBNC are explicitly studied, data for TBPB from ref 13 are included to assist discussion of the kinetics results.

The paper is organized as follows: In section II, a brief account of our experimental technique and theoretical approach is given. In section III, we present the UV−vis spectra of the reacting species, the primary experimental data, that is, the time-resolved results of our pump−probe experiments, and the results from quantum-chemical calculations to be used in section IV. In section IV, we introduce our model for the decarboxylation of carbonyloxy radicals and present the modeling of the measured absorbance versus time profiles, which reflect the time dependence of species concentrations. Subsequently, the influence of molecular structure on both ultrafast decarboxylation via an electronically excited state and thermal decarboxylation via the electronic ground state of carbonyloxy radicals are discussed. Our conclusions are summarized in section V.

II. Experimental Technique and Theoretical Approach

A Ti:sapphire-based regeneratively laser amplified system (VERDI, COHERENT, ORC1000, CLARK), described in more detail elsewhere,[33] delivers 40 fs pulses (800 nm, 0.7 mJ/pulse) at a 1 kHz repetition rate. The laser pulses were split into two parts. The first part, about 30% of total pulse energy, was used for harmonic generation (SHG, THG) of 266 nm pulses for peroxide excitation. The second part serves as a pump pulse for an optical parametric amplifier (TOPAS, Light Conversion). The TOPAS output was frequency-mixed to provide probe pulses in the wavelength range from 290 to 1000 nm. The delay time between pump and probe pulses was set with a computer-controlled translation stage (Newport). Both laser pulses were weakly focused (f = 200 mm) and overlapped spatially and temporally at nearly collinear pump−probe geometry (5°) in a fast-flow cell (0.1−0.2 mm thickness). Pulses with relative polarization at the magic angle (54.7°) were chosen for the experiments. Probe pulse intensities were recorded at a 1 kHz repetition rate in front of and behind the cell, which contained the peroxide solution at an optical density of about 2 (at the pump wavelength). Some of the experiments were carried out with a commercial Ti:sapphire regenerative amplifier system (CPA-2001, Clark-MXR) and two optical parametric amplifiers (TOPAS, Light Conversion and NOPA, Clark-MXR). Whereas

probe pulses for the same wavelength range as above were provided by the TOPAS, tunable pump pulses (230−350 nm) were obtained by second harmonic generation of the NOPA signal. A time resolution of typically 100−200 fs was achieved in solution. The peroxides were synthesized in high purity and kindly provided by AKZO Nobel Polymer Chemicals. Solvents of highest available quality were purchased from Merck. Peroxides and solvents were used without further purification.

As in our previous work on the benzoyloxy radical,[13] density functional theory (DFT) calculations of geometries and energies were performed for isolated phenyloxycarbonyloxy (Ph−O−CO_2), benzylcarbonyloxy (Ph−CH_2−CO_2), and naphthyloxycarbonyloxy (Nph−O−CO_2) radicals. We expect the results for isolated radicals to apply also to radicals in nonpolar and perhaps even weakly polar aprotic solvents, such as the ones employed in our experiments. Details of the quantum-chemical calculations on the three radicals have been published elsewhere.[34] We will here restrict ourselves to a brief account of the procedure and outline only those results for the carbonyloxy radicals that are relevant for the present study. Geometry optimizations were carried out with the DFT variant UB3LYP.[35,36] We used the 6-31G(d), 6-311+G(d,p), 6-311+G(2d,p), and 6-311+G(2df, 2pd) basis sets in the calculations that were carried out employing the Gaussian 98 program package.[37] Three stationary points (reactants, products, and first-order saddle points pertinent to decarboxylation) on the potential energy surface (PES) of each of the radicals were fully optimized using the 6-31G(d) basis set, and the optimized geometries were then refined employing the 6-311+G(d,p) basis. At the obtained structures, additional single-point calculations with the two larger basis sets were carried out. The stationary points were characterized by calculation of the Hessian matrices, and transition-state geometries were further confirmed using the intrinsic reaction coordinate (IRC) method.[38,39] On the basis of comparisons with large-scale coupled-cluster calculations carried out in our previous study,[13] we expect the UB3LYP geometries to be highly reliable. Because the saddle-point structures are very close to the corresponding reactant geometries,[34] the breaking bonds are only slightly elongated and nondynamical electron correlation effects are not expected to play a major role. Thus, the B3LYP functional appears to be an adequate choice for the description of the energetics of the decarboxylations.

III. Results

A. UV/Vis Spectra of Parent Molecules, Intermediates, and Products. Stationary and transient spectra of parent molecules, intermediates, and products will first be discussed. The UV absorption spectra of TBPB in propylene carbonate (PC) solution are given in ref 13, and those of TBPPA, TBPPC, and TBNC are contained in the Supporting Information. Significant UV absorption is found below 300 nm for TBPB, TBPPA, and TBPPC and below 320 nm for TBNC. Excitation at 266 nm into one of the repulsive electronically excited states of these peroxides results in ultrafast direct O−O bond fission.[40] According to Scheme 1, primary dissociation of the peroxides under investigation yields a carbonyloxy/*tert*-butoxy radical pair. The intermediate carbonyloxy radicals subsequently decompose to product radicals (phenyl with TBPB, benzyl with TBPPA, phenyloxy with TBPPC, and naphthyloxy with TBNC) and to CO_2.

In solution, carbonyloxy radicals exhibit a characteristic broad absorption band in the visible to near-infrared region and a sharper absorption component with peak maximum below 450 nm. The spectrum of the benzoyloxy radical has been measured by Misawa et al. in a flash photolysis experiment.[21] On the basis of quantum-chemical calculations, we recently assigned the broad vis−near-IR absorption band of the benzoyloxy radical to the $\tilde{X}^2B_2 \rightarrow \tilde{B}^2A_1$ transition.[13] As detailed in section IVA, the energy of excited states plays a crucial role in determining the contribution of the direct process from an electronically excited state to overall dissociation of the carbonyloxy radicals. Unfortunately, unperturbed transient spectra of the carbonyloxy radicals formed in decomposition of TBPPA, TBPPC, and TBNC have not been reported so far. We expect them to be similar to the spectra of alkyloxycarbonyloxy radicals[41−43] and of other types of carbonyloxy radicals[17,22] because optical transitions in the UV−near-IR spectral region mainly originate from the CO_2 moiety of these radicals.

tert-Butoxy radicals (formed upon primary bond scission of the peroxides) do not show any significant absorption in the near-UV and visible spectral ranges.[13] Radicals formed upon decarboxylation of carbonyloxy radicals (the second step in the sequential decomposition of the organic peroxides discussed here) show significant absorption at wavelengths above 290 nm. The absorption spectrum of the benzyl radical (produced upon decarboxylation of TBPPA) was found to have a maximum at 306 nm at ambient temperature.[44] The matrix spectrum of the phenyloxy radical, as recently reported by Radziszewski et al.,[45,46] has a maximum at 295 nm in argon at 7 K. In addition, phenyloxy radicals show a weak structureless band at around 625 nm. The absorption spectrum of the naphthyloxy radical has not been reported so far. We assume its characteristic features to be similar to those of phenyloxy, apart from a minor red shift caused by the more extended aromatic system.

B. Decarboxylation Measured with Femtosecond Pump−Probe Spectroscopy. The formation of CO_2 after photolysis of TBPPC and TBNC was probed in the IR spectral range with a time resolution of a few picoseconds,[5,30] which is insufficient for obtaining detailed insight into decarboxylation mechanisms. In most cases, intermediate carbonyloxy radicals may be monitored with subpicosecond time resolution in the vis−near-IR spectral range, and product radicals from decarboxylation can be detected in the UV. Absorption of product radicals and carbonyloxy radicals may overlap. We thus measured the transient absorption over a wide UV to near-IR range to identify suitable spectral windows with exclusive or at least predominant absorption of either the intermediate or the product free radical species. It should be noted that time-dependent spectral evolutions due to solvation and vibrational energy transfer (which is always present) are less important here and in previous cases.[5,30] The differences in the features of the time-resolved traces for the different molecules under investigation can be attributed almost exclusively to spectral overlap of intermediate and product radicals (see section IIIA).

TBPPC Decomposition. After photolysis of TBPPC in propylene carbonate (PC) solution at 266 nm, the transient absorbance was recorded at various probe wavelengths between 290 and 830 nm. Typical experimental traces are shown in Figure 1. The absorbance versus time traces measured in the UV region from 290 to 320 nm (left column in Figure 1) differ from each other: at 290 nm, after an initial peak, an off-set and no significant temporal change in absorbance is seen, whereas at 297 nm, a slight increase in absorbance occurs. At and above 320 nm, apart from amplitude modulations, an initial rise in absorbance occurs at $t = 0$ ps, which is followed by a decay on a picosecond to nanosecond time scale. The initial peaks at around $t = 0$ ps are in part due to nonlinear artifacts generated in the solvent medium by the pump and probe pulses.

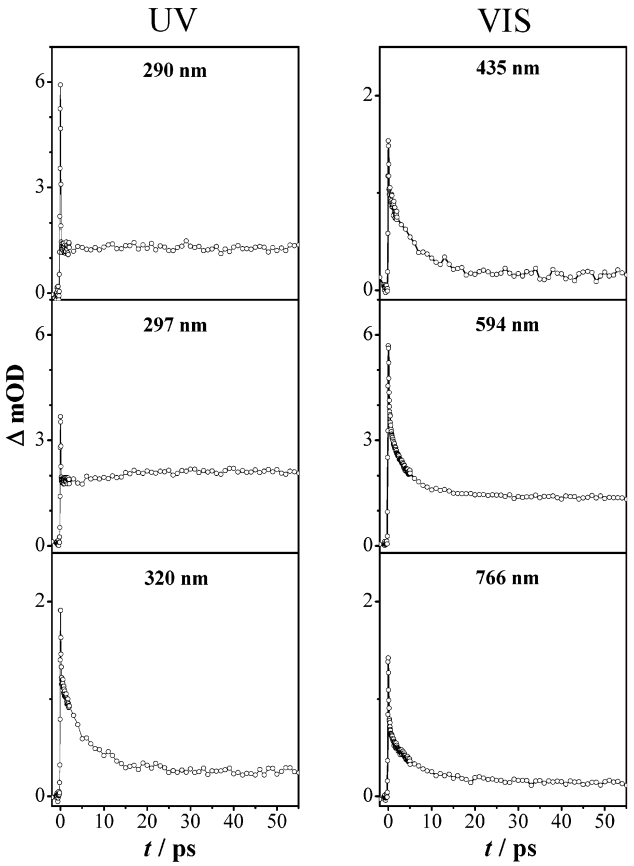

Figure 1. Transient absorbance after photolysis of TBPPC (*tert*-butyl−O−O(O)C−O−Ph) in propylene carbonate solution at 266 nm. Probe wavelengths are indicated.

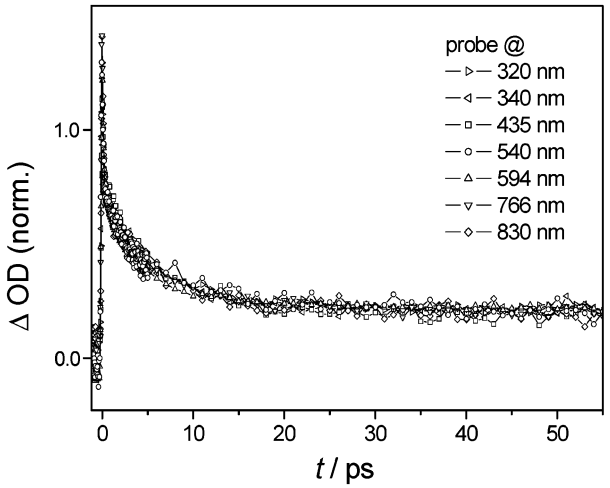

Figure 2. Experimental optical density versus time curves recorded after photolysis of TBPPC in propylene carbonate at 266 nm and probe wavelengths at and above 320 nm. The curves are normalized for better comparison. For further details, see text.

In Figure 2, we compare the traces measured at wavelengths at and above 320 nm. For better comparison, the curves have been normalized by subtraction of an off-set and scaling of the amplitude. The kinetics is very similar throughout the probe region above 320 nm, supporting the assignment of the decay dynamics mostly or even exclusively to the decay dynamics of the phenyloxycarbonyloxy radical. After formation within the experimental time resolution of 100−200 fs, the carbonyloxy radical from TBPPC photolysis decarboxylates on a picosecond to nanosecond time scale. The off-set in absorbance and the absence of a temporal evolution of absorbance at 290 and 297 nm is probably due to overlapping absorption of the (decaying) intermediate phenyloxycarbonyloxy radical and the (rising) phenyloxy product radical. At wavelengths where both species exhibit identical specific absorption, the dynamics may not be detected from the absorbance versus time trace. Because the absorption of the phenyloxy product radical is much stronger in the UV, we expect this compensation in ΔOD to be more pronounced at wavelengths around 295 nm, which is close to the reported maximum of phenyloxy absorbance (see section IIIA). The slight increase in absorbance with time seen at 297 nm (Figure 1) is thus best rationalized as being due to the increase in phenyloxy radical absorbance, dominating over the absorbance of the carbonyloxy radical. We conclude that the unperturbed decarboxylation dynamics in this particular case is best seen in the vis−near-IR region by the observation of the absorbance decay associated with the decrease of intermediate carbonyloxy radical concentration.

TBPPA Decomposition. Examples of optical density versus time traces measured at several wavelengths between 297 and 766 nm after photodissociation (at 266 nm) of TBPPA in PC solution are shown in Figure 3. Again, the temporal behavior of the transient absorption after photolysis of TBPPA strongly depends on the probe wavelength, which indicates absorption contributions of both intermediate and product radicals.

A weak initial increase in absorption is seen at 310 and 320 nm, which wavelengths are close to the reported maximum of the benzyl radical spectrum at 306 nm (see section IIIA). We assume the increase, for example, at 310 nm, to primarily reflect the formation of benzyl radicals in the decomposition of TBPPA.

The experimental trace at 297 nm does not show much temporal change after a few picoseconds. At this wavelength, which is shifted by only about 10 nm to the blue with respect to a reported maximum of the benzyl radical absorbance, we just observe an off-set that is due to absorption of both types of radicals. Toward larger wavelengths (see Figure 3), we observe a picosecond decay in absorption in addition to an off-set. This decay is due to dominant absorption of the carbonyloxy radical, which decarboxylates on a picosecond time scale yielding a benzyl radical and CO_2.

In contrast to TBPPC decomposition, in which all experimental curves above 320 nm exhibit similar absorbance versus time behavior, the situation is more complex with TBPPA decomposition. Between 594 and 700 nm, after an initial peak at $t = 0$ ps, no pronounced temporal change in absorption is seen with the exception of a slight increase or decrease on the picosecond to nanosecond time scales. This behavior is similar to the one observed at a probe wavelength of 297 nm, which we attributed to the simultaneous absorption of the intermediate and the product radical formed upon decomposition of TBPPA. On the other hand, the absorbance at 766 nm clearly shows a picosecond decay similar to the one seen at 330 and 340 nm. Here the carbonyloxy radical is assumed to be dominant in its absorption. In TBPPA decomposition, no region is found where the absorbance may be unambiguously assigned to the carbonyloxy radical. We decided to use the curve measured at 766 nm for analysis of decarboxylation dynamics of the carbonyloxy radical. The reason for this choice is that the absorbance contribution of product radicals is lowest at this wavelength, as can be seen from the small off-set measured at larger reaction times (Figure 3).

TBNC Decomposition. The third molecule investigated is *tert*-butyl-peroxy-2-naphthyl carbonate (TBNC). In the wavelength range above 400 nm, an immediate absorbance increase within

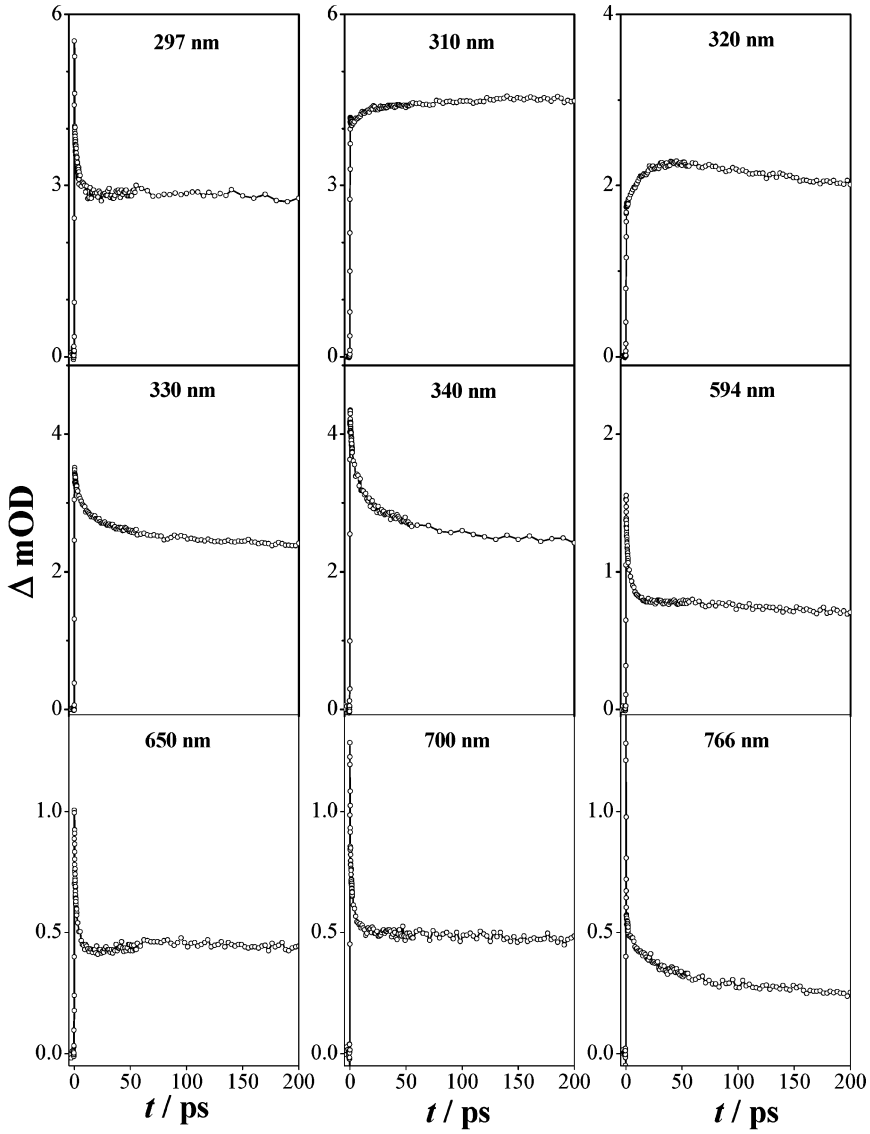

Figure 3. Transient absorbance between 297 and 766 nm after photolysis of TBPPA (*tert*-butyl−O−O(O)C−CH_2−Ph) in propylene carbonate solution at 266 nm. Probe wavelengths are indicated.

less than a picosecond occurs. The subsequent decay on the picosecond time scale is attributed to the absorption of the intermediate 2-naphthyloxycarbonyloxy radical. Characteristic experimental traces for 594 and 766 nm are displayed in Figure 4. The absorption at 297 nm is primarily due to the naphthyloxy product radical.

In Figure 5, we compare normalized experimental absorbance versus time traces recorded after decomposition of TBNC with pump pulses at 266 nm in PC solution. When the different off-sets at $t < 0$ ps and the peak at $t = 0$ ps are ignored, experimental traces throughout the vis−near-IR region show the same time evolution. We assign this decay to the decarboxylation of the intermediate 2-naphthyloxycarbonyloxy radical. Identical decay dynamics of the intermediate carbonyloxy radical are deduced from measurements at the six vis−near-IR wavelengths.

According to the previous arguments for TBPPA, an off-set on the experimental absorbance versus time curves at a particular probe wavelength and for large t is due to absorbance of the product radical. The temporal evolution of the carbonyloxy radical concentration is obtained by its absorbance in the visible region after subtraction of the product radical contribution as measured at large experimental times corresponding to several half-lives of the carbonyloxy radical.

In Figure 6, the naphthyloxy product formation measured at 297 nm and the naphthyloxycarbonyloxy radical decomposition determined at 594 nm are compared. Note that the carbonyloxy radical curve is inverted. The agreement between both curves is very satisfying. Also shown in Figure 6 is the formation of CO_2 as measured by a completely independent IR experiment.[30] As can be seen, the decay of the intermediate 2-naphthyloxycarbonyloxy radicals agrees well with the formation of both products, the 2-naphthyloxy radical and CO_2. The analysis of the CO_2 product concentration further indicates that CO_2 formation has come to completion after 300 ps.[47] The decarboxylation of TBNC after UV excitation thus clearly is a picosecond process even at ambient temperatures. Experiments on the decomposition of TBNC were also carried out in other solvents,[14] and the decarboxylation rate was found to be fairly insensitive toward solvent polarity and viscosity.

C. Quantum-Chemical Calculations. Because of the flatness of the potential energy surfaces in the vicinity of the saddle points pertinent to decarboxylation of the phenyloxy-, benzyl-, and naphthyloxycarbonyloxy radicals, the search for these

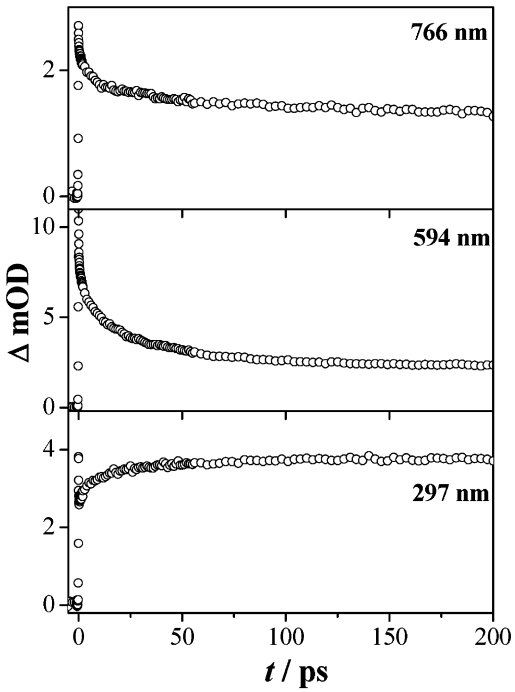

Figure 4. TBNC photolysis at 266 nm in propylene carbonate. Shown is the transient absorption of the naphthyloxycarbonyloxy radical as a function of time at different probe wavelengths of 766 and 594 nm. The trace for 297 nm primarily reflects the absorption of the naphthyloxy radical.

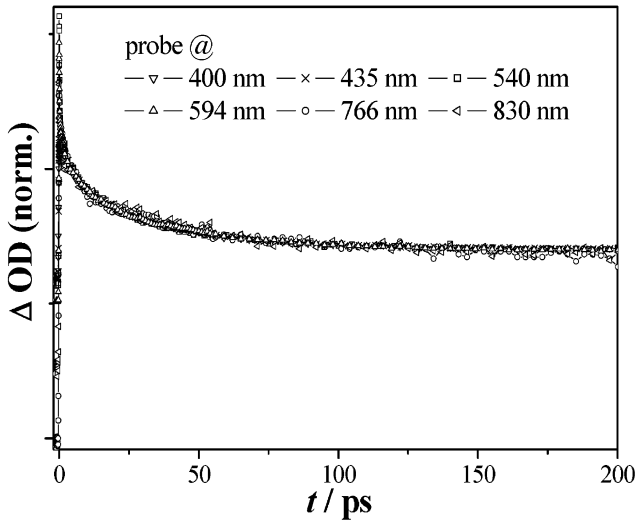

Figure 5. Comparison between experimental traces recorded after decomposition of TBNC at 266 nm in propylene carbonate solution at probe wavelengths in the vis−near-IR region (wavelengths indicated). The curves have been shifted and normalized in intensity for better comparison. The decay dynamics is assigned to the intermediate 2-naphthyloxycarbonyloxy radical.

structures is quite complicated. Because the detailed results of our DFT calculations are reported elsewhere,[34] we here give only a brief account. Reaction energies, $\Delta_R E$, and enthalpies, $\Delta_R H°(298\ K)$, are listed in Table 1. Harmonic vibrational frequencies, ω_i, of the reactant and the saddle-point species are reported in ref 34. They are crucial parameters for the statistical rate constant calculations described in section IV.

Phenyloxycarbonyloxy Radical (Ph−O−CO₂). The results of our UB3LYP/6-311+G(d,p) calculations indicate that the equilibrium reactant and saddle-point geometries of this radical in its $\tilde{X}^2A$ electronic ground state are very close to each other, which is referred to as an "early" transition state. The transition

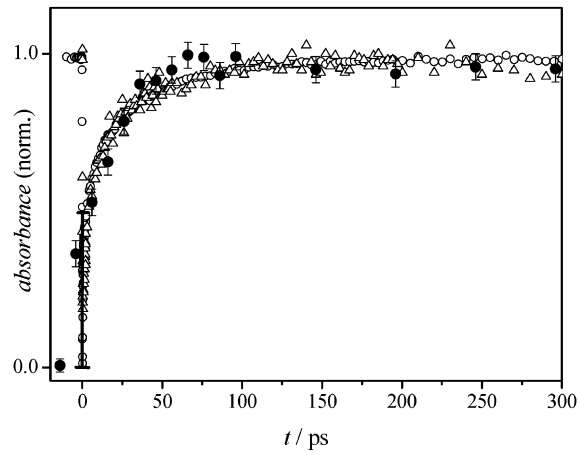

Figure 6. Absorbance change due to the decay of 2-naphthyloxycarbonyloxy radical concentration superimposed onto the formation of 2-naphthyloxy and of CO_2. The data are from different experiments: (○) inverted profile of 2-naphthyloxycarbonyloxy radicals obtained at 594 nm; (△) formation of 2-naphthyloxy radicals at 297 nm; (●) CO_2 absorbance deduced from integrated transient absorption at 4.3 μm during photolysis (308 nm) of TBNC in CCl_4.[30] The bold solid line denotes the yield of direct decarboxylation as described in the text.

TABLE 1: Reaction Energies (in kcal mol^{-1}) for Decarboxylation[a]

carbonyloxy radical	$\Delta_R E$	$\Delta_R H°(298\ K)$
Ph−O−CO_2	−29.7	−30.8
Ph−CH_2−CO_2	−28.3	−29.9
Nph−O−CO_2	−30.6	−31.2

[a] UB3LYP/6-311+G(2df,2pd) results calculated at the UB3LYP/6-311+G(d,p) geometries are given. $\Delta_R E$ denotes the electronic reaction energy; $\Delta_R H°(298\ K)$ is the reaction enthalpy. ZPE and thermal corrections for 298 K were calculated employing the 6-311+G(d,p) basis set.

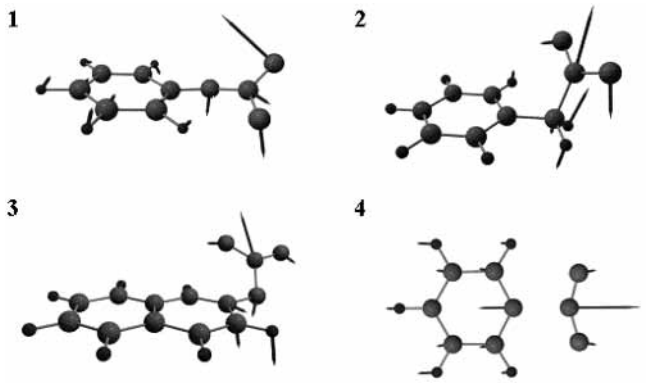

Figure 7. Calculated reactive normal modes at the saddle point for decarboxylation of carbonyloxy radicals: (1) phenyloxycarbonyloxy;[34] (2) benzylcarbonyloxy;[34] (3) naphthyloxycarbonyloxy;[34] (4) benzoyloxy.[13]

mode (normal coordinate with imaginary vibrational frequency) is characterized by a shortening of the Ph−O bond, while the O−CO_2 bond is stretched and eventually broken. Simultaneously, the CO_2 group becomes coplanar with the phenyl ring and attains a linear configuration. The motion is governed by the upper oxygen atom of the CO_2 group (see Figure 7), whereas the displacement vectors of the other two oxygen atoms and of the carboxylic carbon atom are small. Despite the fact that the transition mode seems to end up in a σ-phenoxy radical with the unpaired electron in the ring plane, IRC calculations[34] clearly show that the phenoxy radical is produced in its $\tilde{X}^2B_1$ electronic ground state with the unpaired electron being part of the

delocalized π-system. In a convergence study with respect to basis set size, we calculated the barrier height at the geometry optimized at the UB3LYP/6-311+G(d,p) level of theory employing the large 6-311+G(2d,p) and 6-311+G(2df,2pd) basis sets.[34] After correction of zero-point energy (ZPE), we obtain a barrier height of $E_0 = 2.2$ kcal mol^{-1}.

Benzylcarbonyloxy Radical (Ph−CH$_2$−CO$_2$). The UB3LYP/6-311+G(d,p) results for Ph−CH$_2$−CO$_2$, which are also given in detail in ref 34, indicate that the transition state is very close to the reactant structure ("early" TS). The transition mode is described by a normal coordinate that considerably differs from the case of the Ph−O−CO$_2$ species. Here, the reactive normal coordinate is characterized by a stretching of the CH$_2$−CO$_2$ bond and a simultaneous widening of the CO$_2$ angle, while the Ph−CH$_2$ skeleton is less affected by the reactive normal mode (Figure 7). The CH$_2$ group rotates into the ring plane toward the C_{2v}-symmetric structure of the product benzyl radical. The displacement vector of the carbon atom in the CO$_2$ group clearly dominates the reaction path at the transition state. Visual inspection of the transition mode shows that the benzyl radical is produced in its $\tilde{X}^2B_1$ electronic ground state[48] with the unpaired electron being part of the π-system. The barrier height for decarboxylation, for which we obtain a value of 1.07 kcal mol^{-1}, is only about one-half of that for Ph−O−CO$_2$. It is concluded that substitution of the bridging oxygen atom by a methylene group results in a rather different transition mode for decarboxylation. This is quite surprising because the oxygen atom with its two lone electron pairs should behave similarly to the carbon atom with the attached two hydrogen atoms. Obviously, the bonding situation in phenyloxycarbonyloxy is more complex, and lone pair electrons of the oxygen atom interact with the π-system of the ring.

2-Naphthyloxycarbonyloxy Radical (Nph−O−CO$_2$). The UB3LYP/6-31G(d) calculations for the 2-naphthyloxycarbonyloxy radical yield a very small barrier to decarboxylation, which forced us to use the larger 6-311+G(d,p) basis set to obtain a meaningful optimized geometry. If the harmonic zero-point vibrational energy is added to the classical potential, the effective (or adiabatic) barrier is calculated to be close to zero. Unfortunately, the small barrier height in this case is below the accuracy of the energy estimates by the applied method. To obtain a reliable value for the barrier height to decarboxylation in Nph−O−CO$_2$, high-level quantum dynamical calculations have to be performed, which are out of reach at present. As will be shown below, we obtain a barrier height of $E_0 = (2.9 \pm 0.1)$ kcal mol^{-1} from the analysis of our experimental data.

Our examination reveals that the Nph−O−CO$_2$ geometry differs markedly from the structure of Ph−O−CO$_2$. Most of the geometrical parameters in the saddle-point structure are only very slightly changed with respect to the reactant species, indicating, as expected, again an "early" transition state. The transition mode differs considerably from the Ph−O−CO$_2$ counterpart. While in the latter case the outer carboxylic oxygen atom dominates the normal mode, the motion of the carboxylic carbon atom is most pronounced with Nph−O−CO$_2$ (see Figure 7). The O−CO$_2$ bond stretches, along with a simultaneous widening of the O−C−O angle, and the Nph−O bond becomes shorter. In summary, substitution of the phenyl chromophore by a naphthyl unit should result in significantly different decarboxylation dynamics.

Comparison with the Benzoyloxy Radical (Ph−CO$_2$). As compared with the results for the benzoyloxy radical,[13] the three systems studied in the present paper show significant differences: the carboxylic C−O bond distances of the benzoyloxy radical are markedly longer than those with the other radicals. The O−C−O bond angle, on the other hand, is similar for all species with the exception of Nph−O−CO$_2$ in which this angle is enlarged by about 10°. While the X−CO$_2$ bond distances are shortest for the two aryloxycarbonyloxy radicals (X = O) and longest for the benzylcarbonyloxy species with its pure σ-type bonding situation, benzoyloxy exhibits an intermediate situation. Furthermore, whereas the three saddle-point structures of this work can be classified as "early" transition states, the saddle point in benzoyloxy is shifted much more to the product side. At 8.4 kcal mol^{-1},[13] the barrier for decarboxylation of the benzoyloxy radical is much higher than those for the other three radicals. The reason for this behavior may be found in the strong π-electron delocalization in the planar C_{2v}-symmetric benzoyloxy system.

To shed some light on the structure dependence of the decarboxylation of carbonyloxy radicals from a theoretical perspective, the particular motions of atoms in the normal modes corresponding to the transition modes may be inspected (see Figure 7). In the case of the benzoyloxy radical decarboxylation, the transition mode is governed by a strong motion of the carbon atom of the CO$_2$ moiety. The motions of atoms at the saddle points pertinent to decarboxylation are similar for the benzylcarbonyloxy and naphthyloxycarbonyloxy radicals. In both cases, the decarboxylation is dominated by the motion of the carbon atom of the CO$_2$ group. In contrast to the benzoyloxy radical, the oxygen atoms move in opposite directions so that the formation of linear CO$_2$ does not involve large changes in the X−CO$_2$ (X = O, CH$_2$) bond distances. The decarboxylation dynamics of benzylcarbonyloxy and naphthyloxycarbonyloxy radicals are similar, which is in agreement with our experimental findings.

IV. Discussion

A. Modeling Sequential Decomposition of Peroxides. Concerted breaking of two different bonds of a peroxyester (to yield CO$_2$) after excitation at wavelengths between 250 and 300 nm into the repulsive S_1 state[49] is rather unlikely as has been pointed out in our recent paper.[13] Due to the different nature of the chemical bonds involved, fast sequential dissociation is supposed to be the common decomposition pathway of arylperoxyesters and diaroyl peroxides.[32] Our model, which allows for a quantitative prediction of the decarboxylation dynamics of benzoyloxy radicals from decomposition of TBPB,[13] assumes that after absorption of a photon the peroxide decomposes within one vibrational period and generates a vibrationally excited carbonyloxy radical either in the $\tilde{X}$ ground state or in an electronically excited state. The second fragment, which may also be vibrationally hot, is not detected in our experiments. A ground- ($\tilde{X}$) to excited-state transition in the near-IR range has been used to probe the ground-state population of carbonyloxy radicals.[13]

Electronically excited carbonyloxy radicals are supposed to react in a fast barrierless "downhill reaction" to products, as is depicted in Figure 8. We identified the electronically excited state leading to direct decarboxylation of benzoyloxy radicals as produced in TBPB decomposition to be the $\tilde{B}^2A_1$ state.[13] For carbonyloxy radicals, which exhibit no symmetry elements (thus belonging to point group C_1), such as the ones of the present study, the specific type of electronically excited states involved may not be unambiguously assigned, and no symmetry correlations between carbonyloxy and product radical states can be established. However, coupling between the states is assumed to be sufficiently strong to ensure that reaction takes place

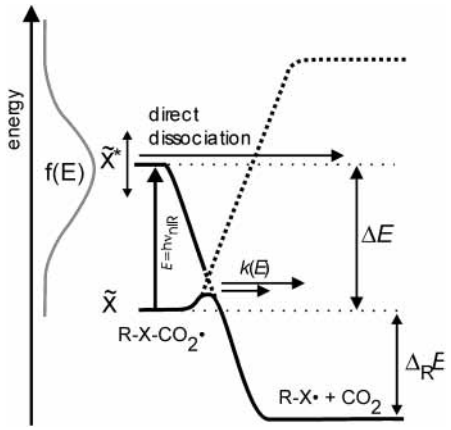

Figure 8. Schematic potential energy diagram by which the two decarboxylation pathways of excited carbonyloxy radicals R−X−CO_2 are illustrated. R is phenyl or naphthyl, and X is O or CH_2. $f(E)$ denotes a particular initial energy distribution of the carbonyloxy radical, $k(E)$ is the specific rate constant for decarboxylation of the intermediate radical, ΔE denotes the energy separation between the electronic ground and the relevant electronically excited state of the carbonyloxy radical, and $\Delta_R E$ is the reaction energy for dissociation into CO_2 and a product radical R−X. For further details, see the text.

whenever sufficient excess energy for a particular reaction channel is available. Depending on the particular reaction channel, that is, whether the decarboxylation takes place exclusively on the ground-state PES or also involves electronically excited states, CO_2 is generated at different initial excess energies, which may be monitored in transient picosecond IR experiments.[5,30,31]

The contribution of immediate carbonyloxy fragmentation from the electronically excited state to overall fragmentation crucially depends on the location of the excited-state energy level with respect to the initial energy of the carbonyloxy radical as represented by the function $f(E)$. For some diaroyl peroxides, such as di(1-naphthoyl) peroxide and di(4-methoxy-benzoyloxy) peroxide, the electronically excited-state level of the intermediate radical is too high to be populated to any relevant extent after peroxide photolysis at 266 nm.[14] With these species, carbonyloxy fragmentation occurs exclusively on the ground-state PES. The process may be adequately treated by statistical unimolecular rate theory.[50]

Our model assumes, first, that the initial excess energy of the peroxide molecule is statistically distributed between the two fragments and, second, that the internal energy of the intermediate radical is statistically distributed over all intramolecular vibrational modes. Microcanonical reaction rate constants for the decarboxylation of carbonyloxy radicals at energy E are calculated via eq 1:[50]

$$k(E) = \frac{W^{\ddagger}(E - E_0)}{h\rho(E)} \tag{1}$$

with $W^{\ddagger}(E - E_0)$ and $\rho(E)$ being the number of energetically accessible transition-state energy levels and the density of reactant states at energy E, respectively. The latter two quantities may be calculated in the rigid-rotor and harmonic-oscillator approximation using barrier heights, E_0, and reactant and transition-state frequencies available from DFT calculations (see above). The thermal time-dependent rate constant is given by averaging over the time-dependent energy distribution, $f(E,t)$:

$$k(t) = f_{\text{rot}} \int_0^{\infty} f(E,t) k(E)\, \mathrm{d}E \tag{2}$$

The function $f(E,t)$ represents the time-dependent "decay" of the initial energy distribution $f(E,t = 0)$ being given by

$$f(E,t{=}0) = \frac{\rho(E) \exp\left(-\frac{E}{k_B T}\right)}{Q_{\text{vib}}} \tag{3}$$

Q_{vib} is the molecular partition function, and T is the initial temperature of the carbonyloxy radical after photolysis of the corresponding peroxide precursor.

The factor f_{rot} in eq 2 is introduced to account for rotational effects on the reaction:

$$f_{\text{rot}} = \sqrt{\prod_{i=1}^{3} B_i / B_i^{\ddagger}} \tag{4}$$

with B_i and $B_i^{\ddagger}$ being the rotational constants of the reactant and transition-state species on the electronic ground-state PESs of carbonyloxy radicals, respectively. These quantities are calculated from the optimized DFT geometries. While the change in rotational constants is negligible for naphthyloxycarbonyloxy radicals with $f_{\text{rot}} = 1.00$ and very small for benzylcarbonyloxy radicals with $f_{\text{rot}} = 1.02$, it becomes somewhat more pronounced for phenyloxycarbonyloxy and benzoyloxy radicals, $f_{\text{rot}} = 1.04$ and $f_{\text{rot}} = 1.06$, respectively.

Intermolecular vibrational energy transfer was globally taken into account by assuming first-order relaxation of $f(E,t)$ with an overall phenomenological relaxation time, $\tau_{\text{VET}} = (7.5 \pm 1.5)$ ps, as observed for molecules of similar complexity and of a similar number of vibrational degrees of freedom.[51] τ_{VET} was kept constant for all molecules dissolved in propylene carbonate. For less-efficient solvents, such as CCl_4, τ_{VET} was selected to be 10 ps. Decay curves, $S(t)_{\text{norm}}$, have been calculated via eq 5

$$S(t)_{\text{norm}} = A(t)\, \mathrm{e}^{-k(t)t} \tag{5}$$

We used a stepladder model for the calculation of $S(t)_{\text{norm}}$, analogous to a master-equation formulation as given in ref 13. The decay curve was simulated using a stepwise procedure for time intervals Δt at constant internal energy E. Energy relaxation was taken into account after each time interval Δt. The optimum size of an individual simulation time interval was found to be $\Delta t = 10$ fs. A scaling factor $A(t)$ was calculated in each iteration step, which ensures a continuous profile for connection of the individual time slices. Prior to comparison with the experimental data, the simulated decay curves, $S(t)_{\text{norm}}$, have been convoluted with the experimental cross-correlation function.

B. Simulation of Time-Resolved Carbonyloxy Radical Concentrations. *Phenyloxycarbonyloxy Radical from TBPPC Decomposition.* The time evolution of the concentration of phenyloxycarbonyloxy radicals is unambiguously deduced from the visible spectral region. Off-sets due to contributions of other species in this region are small and will be neglected in our analysis of the experimental curves. In Figure 9, experimental traces and simulations (solid line) are given for the time evolution of the phenyloxycarbonyloxy radical from TBPPC photolysis between 257 and 266 nm in solvents of different viscosity and polarity. As has been mentioned above, the "spike" on the signal at around $t = 0$ ps is mainly due to a coherence artifact (here only present in PC as a solvent), which occurs on the time scale of the cross-correlation of our experiment, shown by the inset in Figure 9.

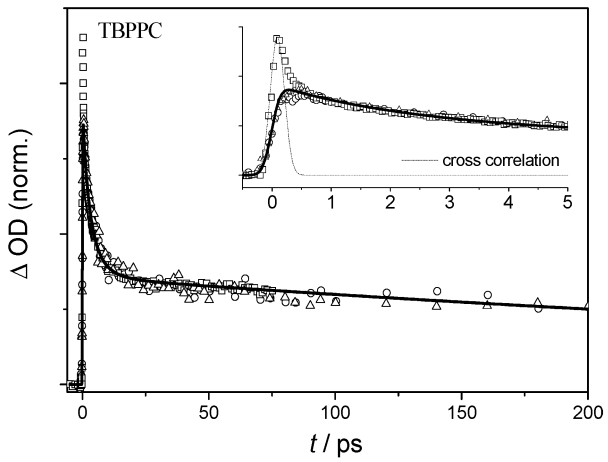

Figure 9. Simulation of the transient absorption of phenyloxycarbonyloxy radicals during photoinduced decomposition of TBPPC in acetonitrile (△, 257 nm pump/620 nm probe), *n*-heptane (○, 257 nm pump/600 nm probe), and propylene carbonate (□, 266 nm pump/594 nm probe). The solid line (—) represents the simulation as described in the text with the parameters $\langle E_{vib}\rangle = 7100$ cm^{-1}, $E_0 = 4.3$ kcal mol^{-1}, and $\tau_{VET} = 7.5$ ps.

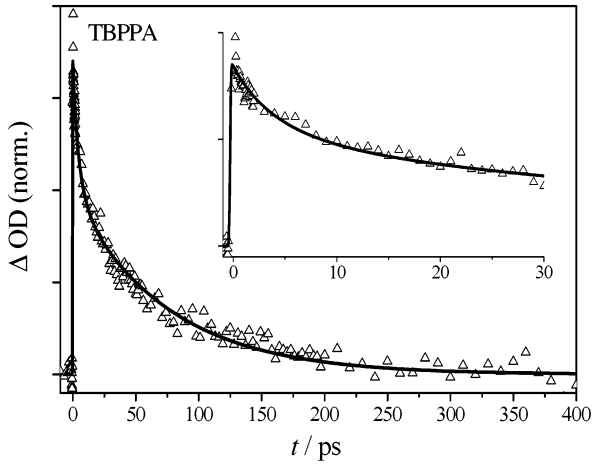

Figure 10. Normalized absorption of benzylcarbonyloxy radicals (△) at 766 nm during photoinduced (266 nm) decomposition of TBPPA in propylene carbonate (contributions due to the product benzyl radical have been subtracted). The solid line (—) represents the simulation of benzylcarbonyloxy radical decarboxylation with the parameters $\langle E_{vib}\rangle = 3000$ cm^{-1}, $E_0 = 3.3$ kcal mol^{-1}, and $\tau_{VET} = 7.5$ ps. For further details, see the text.

Because accurate estimates of barrier height, E_0, are complicated because of the flatness of the PES in the saddle-point region (see section IIIC), we treated E_0 as a fit parameter. Energy transfer to the solvent is taken into account by a time constant, τ_{VET}.[13] The barrier height may be accurately obtained by fitting the ΔOD vs *t* data at larger delay times, which part of the experimental traces reflects the thermal decarboxylation of carbonyloxy radicals at ambient temperature. The best fit was obtained with $E_0 = (4.3 \pm 0.1)$ kcal mol^{-1}, which is reasonably close to the value deduced from our DFT calculations (2.2 kcal mol^{-1}). We simulated the decarboxylation of the carbonyloxy radical on its ground-state PES with different initial internal vibrational energies and found that a value of $\langle E_{vib}\rangle = 7100$ cm^{-1}, corresponding to a vibrational temperature of 720 K, yields very satisfying agreement with the experimental data at early delay times. The uncertainty associated with the relaxation time constant of $\tau_{VET} = (7.5 \pm 1.5)$ ps results in an uncertainty of up to 100 K for the initial temperature of the carbonyloxy radicals.

The total internal energy of phenyloxycarbonyloxy radicals that is instantaneously available at $t = 0$ with TBPPC photolysis at 257 and 266 nm may be estimated from the reaction enthalpy of peroxide dissociation into the two primary radicals, which was determined to be 23.0 kcal mol^{-1} at 298 K (UB3LYP/6-311+G(2d,p)). The obtained initial energies of 15 300 cm^{-1} (257 nm excitation) and 14 600 cm^{-1} (266 nm excitation) correspond to temperatures of 1130 and 1100 K, respectively, which are almost twice as high as the value found from simulation of the statistical ground-state reaction. This discrepancy may be explained by a significant contribution of ultrafast phenyloxycarbonyloxy decarboxylation via an electronically excited state. The latter reaction depletes the high-energy part of the phenyloxycarbonyloxy radical population on a subpicosecond time scale. The remaining radicals react statistically on the ground-state PES. This interpretation is consistent with the observation from previous picosecond IR experiments that the produced CO_2 has high initial internal vibrational energy at time *t* being close to zero.[5] The branching ratio of decarboxylation via an electronically excited state to decarboxylation on the ground-state potential energy surface may be estimated from both CO_2 excess energies and initial internal energies available for ground-state decarboxylation of carbonyloxy radicals. The decarboxylation of the phenyloxycarbonyloxy radical after TBPPC excitation at 266 nm in propylene carbonate is estimated to proceed with (50 ± 30)% via an electronically excited state.

Benzylcarbonyloxy Radical Decarboxylation from TBPPA Decomposition. According to the observed decay of the intermediate benzylcarbonyloxy radical (dominant absorption at, for example, 766 nm) and in agreement with our quantum-chemical calculations, the decarboxylation dynamics has been found to be a picosecond process. Figure 10 shows experimental and simulated traces for the decarboxylation dynamics of the benzylcarbonyloxy radical. The experimental signal is obtained by subtraction of the benzyl radical contribution at 766 nm measured at large delay times.

A barrier height of $E_0 = (3.3 \pm 0.1)$ kcal mol^{-1} was used in the simulation, which number is in reasonable agreement with the value from our quantum-chemical calculations (1.07 kcal mol^{-1}). We determined the rate constant for the thermal decarboxylation of benzylcarbonyloxy radicals at 300 K to be $k = 1.3 \times 10^{10}$ s^{-1}. With an initial internal vibrational energy of the ground-state benzylcarbonyloxy radical of $\langle E_{vib}\rangle = 3000$ cm^{-1}, corresponding to an internal temperature of 450 K, satisfactory agreement between experiment and simulation is obtained (see Figure 10). The total initial internal energy of the benzylcarbonyloxy radical available after 266 nm photolysis of TBPPA is estimated using $\Delta_R H°(298\ K) = 24.7$ kcal mol^{-1} (calculated at UB3LYP/6-311+G(2d,p)). One obtains an initial energy of 15 000 cm^{-1}, corresponding to an initial temperature of 1050 K. As compared to TBPPC decomposition, the discrepancy between (estimated) initial total internal energy and initial vibrational energy of the benzylcarbonyloxy radical, as obtained from kinetic modeling, is even larger with TBPPA. This suggests that direct decarboxylation from the excited-state plays an even more important role. The contribution is estimated to be (75 ± 20)%. This value is in agreement with the large instantaneous absorbance change as compared to the subsequent minor time-dependent change observed in the spectral trace taken at 310 nm (see Figure 3).

Our findings are in agreement with what has been reported on the thermal decomposition of TBPPA,[7−12] for which a close-to-concerted decarboxylation mechanism was postulated. Bockman et al. studied the decarboxylation of benzylcarbonyloxy

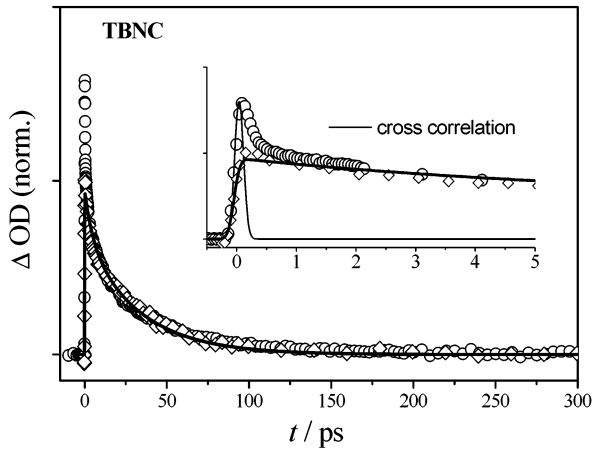

Figure 11. Normalized transient absorption of 2-naphthyloxycarbonyloxy radicals during photoinduced decomposition of TBNC in *n*-heptane (◇, 282 nm pump/600 nm probe) and propylene carbonate (○, 266 nm pump/594 nm probe). The solid line (—) represents the simulation as described in the text with the parameters $\langle E_{vib}\rangle = 2700$ cm^{-1}, $E_0 = 2.9$ kcal mol^{-1}, and $\tau_{VET} = 7.5$ ps. For further details, see text.

and similar carbonyloxy radicals by femtosecond visible spectroscopy[28] and found a rate constant of $k = 1.6 \times 10^9$ s^{-1} for the decarboxylation of benzylcarbonyloxy radicals in water. Hilborn and Pincock report a unimolecular rate constant of $k = 5 \times 10^9$ s^{-1} for the decarboxylation of benzylcarbonyloxy radicals in methanol.[52] It is however not clear whether these data[28,52] are suitable for comparison with the ones from our study in a weakly interacting solvent environment.

2-Naphthyloxycarbonyloxy Radical Decarboxylation from TBNC Decomposition. Fast decarboxylation on a picosecond time scale is also seen for the 2-naphthyloxycarbonyloxy radical generated in the photolysis of TBNC in solution. Figure 11 shows the decarboxylation dynamics of this radical as measured at 594 nm in PC and at 600 nm in *n*-heptane after subtraction of the contribution of the product radical (measured at 297 nm and normalized in intensity to represent the ΔOD values at 300 ps of the curves around 600 nm). The decarboxylation of 2-naphthyloxycarbonyloxy radicals, formed upon decomposition of TBNC at UV wavelengths, occurs in a similar way as does the decarboxylation of benzylcarbonyloxy radicals. The decarboxylations are found to be highly exothermic for both carbonyloxy radicals and involve a low reaction barrier. This is consistent with our DFT calculations, which gave low barrier values for the decarboxylation for benzylcarbonyloxy and for 2-naphthyloxycarbonyloxy radicals. Assuming these barriers to be correct means that decarboxylation of both carbonyloxy radicals is a picosecond process even at ambient temperature (see Figure 11).

The decarboxylation of 2-naphthyloxycarbonyloxy radicals was simulated using vibrational frequencies and rotational constants from our UB3LYP calculations.[34] Fitting of the experimental data yields a barrier of $E_0 = (2.9 \pm 0.1)$ kcal mol^{-1}, which is the lowest barrier value found for the investigated R−X−CO_2 radicals, in agreement with the trend in our calculations. Under the particular photodecomposition conditions, the initial internal energy of the 2-naphthyloxycarbonyloxy radical was deduced to be $\langle E_{vib}\rangle = 2700$ cm^{-1}, corresponding to an initial temperature of 370 K. The decarboxylation was also measured in *n*-heptane solution after excitation of TBNC at 282 nm (see Figure 11). When the artifact at $t = 0$ ps in PC solution is ignored, the results indicate that the excitation wavelength does not significantly change the observed temporal evolution. This can be easily understood in terms of our model: within the first 5 to 10 ps, we observe the ground-state reaction of 2-naphthyloxycarbonyloxy radicals with a modest excess internal energy corresponding to about 370 K. After equilibration to ambient temperature with a time constant of about (7.5 ± 1.5) ps, the thermal decarboxylation at ambient temperature is seen. Measurements in different solvents[14] demonstrate that the latter process is affected neither by solvent viscosity nor by polarity (e.g., *n*-heptane and PC as solvents do not result in any significant change of decarboxylation dynamics, see Figure 11). With an enthalpy of reaction, $\Delta_R H°$(298 K), of 19.7 kcal mol^{-1}, as calculated by UB3LYP/6-311+G(d,p)//6-31G+(d,p), the initial internal energy of 2-naphthyloxycarbonyloxy radicals after photodissociation of the peroxide at wavelengths between 257 and 308 nm is estimated to be 15 500−19 500 cm^{-1}, which corresponds to initial temperatures in the range 900−1030 K. The initial internal energy of carbonyloxy radicals monitored in their respective ground state is much lower than predicted by statistical estimates. This observation suggests a large contribution of direct decarboxylation of the intermediate 2-naphthyloxycarbonyloxy radical via an electronically excited state. The contribution of direct decarboxylation is estimated from the amplitude ratio of prompt versus delayed product formation as seen in Figure 6 (indicated by the bold solid line representing the contribution of direct decarboxylation) to be (50 ± 20)%. This percentage is consistent with the value deduced from depletion of the high-energy tail of the initial energy distribution of intermediate radicals and with high excess energies of the CO_2 product found in previous picosecond IR experiments.[5]

C. Dependence of the Decarboxylation Kinetics on Peroxide Structure. Our experiments on various peroxides indicate that the ultrafast decarboxylation kinetics is clearly related to the structure of the parent peroxide molecule. However, a clear trend of the variations in time-resolved traces upon chemical substitution is difficult to identify. According to the pioneering work by Bartlett and Hiatt,[6] the structural dependence of the decarboxylation dynamics results, at least in part, from different stabilities of the product radicals. Our calculations indicate an increase in exothermicity of the decarboxylation step by about 30 kcal mol^{-1} in going from R−CO_2 to R−X−CO_2. According to the Bell−Evans−Polanyi principle,[53,54] this trend is accompanied by a lowering of barrier height. This effect may also account for the variation in the empirical barrier values deduced from the modeling of experimental decarboxylation data of carbonyloxy radicals, R−X−CO_2. Unfortunately, the accurate prediction of the small barrier heights by DFT calculations turned out to be more difficult than that in cases where the barrier is high.[14] The relative size of barrier heights is, however, well reproduced by our quantum-chemical calculations.

In addition to the effect of barrier height, the different contributions of electronically excited states to overall decarboxylation that originate from chemical (structural) modification probably play an important role. These contributions are by far more significant than those resulting from changes in frequencies and in the nature of the transition modes (147*i* cm^{-1} for Ph−O−CO_2 decarboxylation, 257*i* cm^{-1} for Nph−O−CO_2, 795*i* cm^{-1} for Ph−CH_2−CO_2 decarboxylation,[34] and 253*i* cm^{-1} for the benzoyloxy radical[13]). In fact, the differences in the rate constants of more than 3 orders of magnitude between, for example, Ph−CO_2 and Nph−O−CO_2 decarboxylation (see Table 2) can obviously not be explained solely in terms of differences in transition modes.

TABLE 2: Arrhenius Parameters, A and E_a, as Deduced from a Fit of Temperature-Dependent Rate Constants between 200 and 2000 K Estimated via Transition-State Theory

carbonyloxy radical	A (10^{13} s^{-1})	E_a (kcal mol^{-1})	k(300 K) (s^{-1})
$Ph-CO_2$	7.66	9.44	1.0×10^7
$Ph-O-CO_2$	0.59	4.83	1.8×10^9
$Ph-CH_2-CO_2$	0.97	3.94	1.3×10^{10}
$Nph-O-CO_2$	0.75	3.29	3.0×10^{10}

A general *quantitative* understanding of the structure dependence or predictive power will certainly benefit from additional experimental and theoretical investigations, in particular on systems with small activation barriers and large excited-state contributions to the dissociation dynamics.

Finally, we would like to point out that data from these photochemically induced measurements in combination with quantum-chemical calculations and kinetic modeling may provide thermal rate constants for the decarboxylation of peroxide molecules. Benzoyloxy radicals in their electronic ground state exhibit a lifetime in the nanosecond to microsecond range and are thus relatively stable toward decarboxylation at ambient temperature, whereas carbonyloxy radicals of general structure $R-X-CO_2$ (R = phenyl or naphthyl, X = O or CH_2) in their electronic ground states are considerably less stable. Table 2 shows kinetic parameters for the decarboxylation of carbonyloxy radicals. To deduce these numbers, temperature-dependent *thermal* rate constants within the range 200−2000 K have been calculated employing transition-state theory on the basis of our experimentally determined barrier heights and quantum-chemical calculations. These rate coefficients have been fitted to an Arrhenius-type expression, $k(T) = A \exp(-E_a/(RT))$, to obtain the parameters A and E_a listed in Table 2.

These thermal rate constants from ultrafast photoinduced dissociation experiments should be very helpful for estimating *thermally activated* decomposition rate of peroxides over a very wide time scale.

V. Conclusions

The decarboxylation of carbonyloxy radicals in solution from laser light-induced decomposition of organic peroxides of general structure R−X−C(O)O−O−*tert*-butyl with R = phenyl and X = O (TBPPC), R = phenyl and X = CH_2 (TBPPA), and R = naphthyl and X = O (TBNC) has been studied by absorption spectroscopy on a picosecond time scale. The decarboxylation kinetics is compared with recently published data for *tert*-butyl peroxybenzoate (Ph−C(O)O−O−*tert*-butyl, TBPB) decomposition.[13] Thermally equilibrated benzoyloxy radicals decarboxylate on a nanosecond to microsecond time scale. In contrast, carbonyloxy radicals from UV photolysis of TBPPA, TBPPC, and TBNC decarboxylate at much faster rates in the picosecond time domain. The decarboxylation rate on the ground-state PES of the carbonyloxy radicals increases in the order phenyl−C(O)O−(O−*tert*-butyl) < phenyl−O−C(O)O−(O−*tert*-butyl) < phenyl−CH_2−C(O)O−(O-*tert*-butyl) < naphthyl−O−C(O)O−(O−*tert*-butyl).

With barrier heights and vibrational frequencies of the carbonyloxy radicals obtained from DFT calculations for both reactant states and saddle-point geometries, we have used our recently proposed model to simulate the decarboxylation dynamics. The observed order of decarboxylation rates of the studied peroxides is consistent with model predictions based on UB3LYP calculations. In addition, our analysis provides evidence for a significant contribution to overall decarboxylation of an ultrafast excited-state decarboxylation channel of initially highly excited carbonyloxy radicals. Low barrier heights toward decarboxylation of carbonyloxy radicals are associated with large reaction contributions via excited states of these radicals, which suggests that the energy gap between ground and excited states is small for less-stable carbonyloxy radicals. Direct decarboxylation might occur via the first electronically excited state in these carbonyloxy radicals, which is known to be energetically close to the electronic ground state. In support of this conclusion, a recent study[55] on the highly exothermal decarboxylation of 9-methylfluorenylcarbonyloxy radicals generated via UV photolysis of *tert*-butyl 9-methylfluorene-9-percarboxylate, which exhibit a lifetime of only 55 ps in ambient temperature solutions,[24] provides evidence for a significant contribution of an excited-state channel to the reaction.

The detailed analysis of the photoinduced decomposition of organic peroxides also allows us to estimate Arrhenius parameters for thermal decarboxylation rate constants, $k(T)$, of carbonyloxy radicals. These rate coefficients are important quantities for deducing initiator efficiencies of peroxides in free-radical polymerizations. The correlation between peroxide structure and decomposition kinetics is a key feature for selecting suitable peroxide initiators.

Acknowledgment. The authors acknowledge financial support by the Deutsche Forschungsgemeinschaft (DFG) within Sonderforschungsbereich 357 ("Molekulare Mechanismen Unimolekularer Prozesse") and from the Fonds der Chemischen Industrie. We are grateful to AKZO-Nobel Polymer Chemicals (Deventer) for preparing and kindly providing the peroxide samples. We thank Dipl.-Chem. J. Zerbs for experimental support and Dr. R. Oswald for his help with preparing Figure 7. We also enjoyed stimulating discussions about various aspects of this work with Professors P. Botschwina and J. Troe.

Supporting Information Available: Linear absorption spectra for *tert*-butyl peroxyphenyl carbonate (TBPPC), *tert*-butyl peroxyphenylacetate (TBPPA), and *tert*-butyl peroxy-2-naphthyl carbonate (TBNC) between 220 and 340 nm. This material is available free of charge via the Internet at http://pubs.acs.org.

References and Notes

(1) Fujimori, K. In *Organic Peroxides*; Ando, W., Ed.; Wiley: New York, 1992; p 319.
(2) Sawaki, Y. In *Organic Peroxides*; Ando, W., Ed.; Wiley: New York, 1992; p 425.
(3) Barson, C. A.; Bevington, J. C. *J. Polym. Sci., Part A: Polym. Chem.* **1997**, *35*, 2955.
(4) Buback, M.; Sandmann, J. *Z. Phys. Chem.* **2000**, *214*, 583.
(5) Buback, M.; Kling, M.; Seidel, M. T.; Schott, F.-D.; Schroeder, J.; Steegmüller, U. *Z. Phys. Chem.* **2001**, *215*, 717.
(6) Bartlett, P. D.; Hiatt, R. R. *J. Am. Chem. Soc.* **1958**, *80*, 1398.
(7) Bartlett, P. D.; Simons, D. M. *J. Am. Chem. Soc.* **1960**, *82*, 1753.
(8) Bartlett, P. D.; Rüchardt, C. *J. Am. Chem. Soc.* **1960**, *82*, 1756.
(9) Koenig, T.; Wolf, R. *J. Am. Chem. Soc.* **1967**, *89*, 2948.
(10) Koenig, T.; Wolf, R. *J. Am. Chem. Soc.* **1969**, *91*, 2574.
(11) Pryor, W. A.; Smith, K. *J. Am. Chem. Soc.* **1970**, *92*, 5403.
(12) Neuman, R. C.; Behar, J. V. *J. Am. Chem. Soc.* **1969**, *91*, 6024.
(13) Abel, B.; Assmann, J.; Botschwina, P.; Buback, M.; Kling, M.; Oswald, R.; Schmatz, S.; Schroeder, J.; Witte, T. *J. Phys. Chem. A* **2003**, *107*, 5157.
(14) Assmann, J.; Kling, M.; Abel, B. *Angew. Chem., Int. Ed.* **2003**, *42*, 2226.
(15) Chateauneuf, J.; Lusztyk, J.; Ingold, K. U. *J. Am. Chem. Soc.* **1988**, *110*, 2877.
(16) Hashimoto, J.; Segawa, K.; Sakuragi, H. *Chem. Phys. Lett.* **1999**, *314*, 261.
(17) Wang, J.; Tateno, T.; Sakuragi, H.; Tokumaru, K. *J. Photochem. Photobiol.* **1995**, *92*, 53.

(18) Yamauchi, S.; Hirota, N.; Takahara, S.; Sakuragi, H.; Tokumaru, K. *J. Am. Chem. Soc.* **1985**, *107*, 5021.
(19) Yamauchi, S.; Hirota, N.; Takahara, S.; Misawa, H.; Sawabe, K.; Sakuragi, H.; Tokumaru, K. *J. Am. Chem. Soc.* **1989**, *111*, 4402.
(20) Tateno, T.; Sakuragi, H.; Tokumaru, K. *Chem. Lett.* **1992**, *20*, 1883.
(21) Misawa, H.; Sawabe, K.; Takahara, S.; Sakuragi, H.; Tokumaru, K. *Chem. Lett.* **1988**, *23*, 357.
(22) Chateauneuf, J.; Lusztyk, J.; Ingold, K. U. *J. Am. Chem. Soc.* **1988**, *110*, 2886.
(23) Bevington, J. C.; Lewis, T. D. *Trans. Faraday Soc.* **1958**, *54*, 1340.
(24) Falvey, D. E.; Schuster, G. B. *J. Am. Chem. Soc.* **1986**, *108*, 7419.
(25) Morlino, E. A.; Bohorquez, M. D.; Neckers, D. C.; Rodgers, A. A. J. *J. Am. Chem. Soc.* **1991**, *113*, 3599.
(26) Allen, N. S.; Hardy, S. J.; Jacobine, A. F.; Glaser, D. M.; Navaratnam, S.; Parsons, B. J. *J. Photochem. Photobiol., A* **1990**, *50*, 389.
(27) Bockman, T. M.; Hubig, S. M.; Kochi, J. K. *J. Am. Chem. Soc.* **1996**, *118*, 4502.
(28) Bockman, T. M.; Hubig, S. M.; Kochi, J. K. *J. Org. Chem.* **1997**, *62*, 2210.
(29) Abel, B.; Assmann, J.; Buback, M.; Kling, M.; Schmatz, S.; Schroeder, J. *Angew. Chem., Int. Ed.* **2003**, *42*, 299.
(30) Aschenbrücker, J.; Buback, M.; Ernsting, N. P.; Schroeder, J.; Steegmüller, U. *Ber. Bunsen-Ges. Phys. Chem.* **1998**, *102*, 965.
(31) Aschenbrücker, J.; Buback, M.; Ernsting, N. P.; Schroeder, J.; Steegmüller, U. *J. Phys. Chem. B* **1998**, *102*, 5552.
(32) Maul, C.; Gericke, K.-H. *Int. Rev. Phys. Chem.* **1997**, *16*, 1.
(33) Assmann, J.; v. Benten, R.; Charvat, A.; Abel, B. *J. Phys. Chem. A* **2003**, *107*, 1904.
(34) Kling, M.; Schmatz, S. *Phys. Chem. Chem. Phys.* **2003**, *5*, 3891.
(35) Becke, A. D. *J. Chem. Phys.* **1993**, *98*, 5648.
(36) Lee, C.; Yang, W.; Parr, R. G. *Phys. Rev. B* **1988**, *37*, 785.
(37) Frisch, M. J.; Trucks, G. W.; Schlegel, H. B.; Scuseria, G. E.; Robb, M. A.; Cheeseman, J. R.; Zakrzewski, V. G.; Montgomery, J. A., Jr.; Stratmann, R. E.; Burant, J. C.; Dapprich, S.; Millam, J. M.; Daniels, A. D.; Kudin, K. N.; Strain, M. C.; Farkas, O.; Tomasi, J.; Barone, V.; Cossi, M.; Cammi, R.; Mennucci, B.; Pomelli, C.; Adamo, C.; Clifford, S.; Ochterski, J.; Petersson, G. A.; Ayala, P. Y.; Cui, Q.; Morokuma, K.; Malick, D. K.; Rabuck, A. D.; Raghavachari, K.; Foresman, J. B.; Cioslowski, J.; Ortiz, J. V.; Stefanov, B. B.; Liu, G.; Liashenko, A.; Piskorz, P.; Komaromi, I.; Gomperts, R.; Martin, R. L.; Fox, D. J.; Keith, T.; Al-Laham, M. A.; Peng, C. Y.; Nanayakkara, A.; Gonzalez, C.; Challacombe, M.; Gill, P. M. W.; Johnson, B. G.; Chen, W.; Wong, M. W.; Andres, J. L.; Head-Gordon, M.; Replogle, E. S.; Pople, J. A. *Gaussian 98*, revision A.9; Gaussian, Inc.: Pittsburgh, PA, 1998.
(38) Gonzales, C.; Schlegel, H. B. *J. Chem. Phys.* **1989**, *90*, 2154.
(39) Gonzales, C.; Schlegel, H. B. *J. Phys. Chem.* **1990**, *94*, 5523.
(40) Dorer, F. H.; Johnson, S. N. *J. Phys. Chem.* **1971**, *75*, 3651.
(41) Chateauneuf, J.; Lusztyk, J.; Maillard, B.; Ingold, K. U. *J. Am. Chem. Soc.* **1988**, *110*, 6727.
(42) Behar, D.; Czapski, G.; Duchovny, I. *J. Phys. Chem.* **1970**, *74*, 2206.
(43) Chen, S.; Cope, V. W.; Hoffman, M. Z. *J. Phys. Chem.* **1973**, *77*, 1111.
(44) Ikeda, N.; Nakashima, N.; Yoshihara, K. *J. Phys. Chem.* **1984**, *88*, 5803.
(45) Radziszewski, J. G.; Gil, M.; Gorski, A.; Spanget-Larsen, J.; Waluk, J.; Mroz, J. *J. Chem. Phys.* **2001**, *115*, 9733.
(46) Radziszewski, J. G.; Gil, M.; Gorski, A.; Spanget-Larsen, J.; Waluk, J.; Mroz, J. *J. Chem. Phys.* **2002**, *116*, 5912.
(47) Steegmüller, U. Dissertation (Ph.D.), University of Göttingen, Göttingen, Germany, 1997.
(48) Rice, J. E.; Handy, N. C.; Knowles, P. J. *J. Chem. Soc., Faraday Trans. 2* **1987**, *83*, 1643.
(49) Scaiano, J. C.; Wubbels, G. G. *J. Am. Chem. Soc.* **1981**, *103*, 640.
(50) Baer, T.; Hase, W. L. *Unimolecular Reaction Dynamics: Theory and Experiments*; Oxford University Press: New York, 1996.
(51) Schwarzer, D.; Troe, J.; Zerezke, M. *J. Chem. Phys.* **1997**, *107*, 8380.
(52) Hilborn, J. W.; Pincock, J. A. *J. Am. Chem. Soc.* **1991**, *113*, 2683.
(53) Bell, R. P. *Trans. Faraday Soc.* **1937**, *33*, 496.
(54) Evans, M. G.; Polanyi, M. *Trans. Faraday Soc.* **1936**, *32*, 1333.
(55) Abel, B.; Buback, M.; Kling, M.; Schmatz, S.; Schroeder, J. *J. Am. Chem. Soc.*, in press (available in electronic form via the Internet at http://pubs.acs.org).